Science Bulletin 70 (2025) 2739–2742

Contents lists available at ScienceDirect

Science Bulletin

journal homepage: www.elsevier.com/locate/scib

Short Communication

Local regulation and global reconstruction of polar networks in twisted bilayer MoS_2

Jiakai Wang [a], Xu Han [b], Guanchu Liu [b], Zihao Guo [b], Longshuo Gu [a], Jiahao Yan [b], Shiqi Yang [a], Chunsheng Hu [b], Chicheng Liu [b], Yunyun Dai [a,b], Xia Liu [b], Yuan Huang [a,b,*], Yeliang Wang [a,b,*]

[a] School of Physics, Beijing Institute of Technology, Beijing 100081, China
[b] School of Integrated Circuits and Electronics, MIIT Key Laboratory for Low-Dimensional Quantum Structure and Devices, Beijing Institute of Technology, Beijing 100081, China

ARTICLE INFO

Article history:
Received 15 April 2025
Received in revised form 23 May 2025
Accepted 3 June 2025
Available online 21 June 2025

In recent years, two-dimensional (2D) material moiré superlattices have emerged as a research focus in condensed matter physics and materials science due to their unique physical properties [1,2]. These phenomena fundamentally stem from the synergistic interplay between electron correlation effects and topological characteristics under periodic modulation. Among these, moiré polarization [3,4], as a crucial member of the moiré physics family, provides a novel platform for exploring ultrathin ferroelectric responses to external fields due to its unique polarization distribution mechanism and tunability [5,6]. Although many cutting-edge devices are used to characterize and control moiré polar networks, the existing control technologies mostly remain at the macroscopic level [7–14]. The localized regulation mechanisms of ferroelectric domains and their domain walls under external electric fields remain insufficiently understood [15]. Achieving precise electrical control over these artificial moiré superlattices at microscopic scales is not only crucial for unveiling their unique quantum effects, but also holds significant potential for developing next-generation high-density nonvolatile memory devices.

In this study, we systematically examine polarization dynamics in twisted bilayer MoS_2 (tBL-MoS_2) moiré polar networks using piezoresponse force microscopy (PFM) combined with *in situ* electrical manipulation. Owing to PFM's high-resolution characterization capabilities and localized modulation capacity, we have observed phenomena that are elusive to conventional macroscopic characterization methods. Samples are fabricated via the tear-stack technique [16,17]. Experimental results indicate that the polarization evolution of moiré ferroelectric domains under a local electric field is topologically protected. Furthermore, when the moiré polar networks are affected by structural defects, they undergo global reconstruction to preserve their unique polarization distribution. This research provides crucial experimental foundations for optimizing moiré ferroelectric device fabrication and establishes a new paradigm for developing 2D low-power topological memory devices.

Twisted bilayer MoS_2 samples were successfully fabricated using the tear-stack technique. Detailed procedures for material fabrication are provided in Figs. S1 and S2 (online). The test structure comprises a total of five layers (Fig. 1a), with key components including tBL-MoS_2 and graphene. The former induces moiré polarization, while the latter provides a mechanically and electrically favorable environment that ensures robust PFM measurement and reduces the required DC voltage for domain modulation. Subsequent characterization of moiré polar networks in the samples was performed using PFM, as shown in Figs. S3–S5 (online). The moiré polarization exhibits a strict one-to-one correspondence with atomic stacking configurations, primarily comprising four types: XM/MX, MM, and saddle point (SP) (Fig. S4 online). The out-of-plane polarization predominantly originates from the XM/MX stacking, which serves as the primary contributor to moiré polarization and manifests as triangular domains with periodic arrangements. The MM stacking, characterized by a centrosymmetric structure, lacks polarization due to its symmetry constraints. It is commonly referred to as "node" as it typically resides at the vertices of triangular domains. The SP configuration acts as domain wall that separate XM and MX regions, exhibiting coexisting out-of-plane and in-plane polarization.

By selecting regions with specific ferroelectric domains in moiré polar network, and applying a voltage for an adequate duration, precise domain regulation can be achieved (Fig. 1b). Fig. 1c and

* Corresponding authors.
E-mail addresses: yhuang@bit.edu.cn (Y. Huang), yeliang.wang@bit.edu.cn (Y. Wang).

https://doi.org/10.1016/j.scib.2025.06.026
2095-9273/

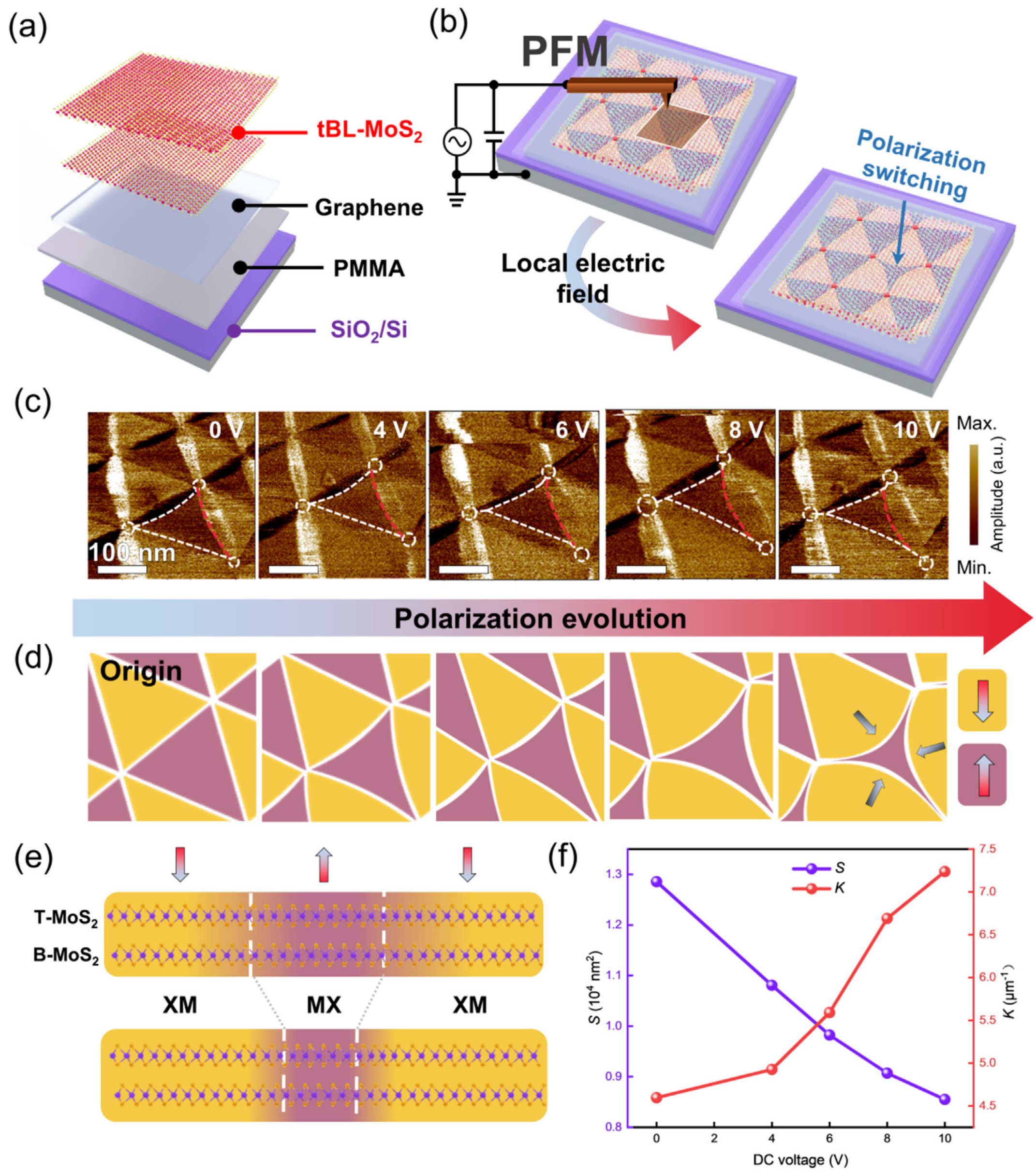

Fig. 1. Polarization evolution in moiré polarization under local electric field. (a) Structural schematic of tBL-MoS_2. (b) Schematic diagram of applying voltage to a local area in the moiré polar network. (c) Amplitude map of triangular ferroelectric domains obtained during a DC bias modulation experiment (0 V, 4–10 V) on the same sample region after averaging, dashed lines indicate the geometric outlines of the domains. Schematic illustration of the polarization evolution mechanism: (d) top view and (e) side view. (f) Quantitative plot of ferroelectric domain area *S* and domain wall curvature *K* under different bias voltages.

Fig. S6 (online) display the evolution of triangular ferroelectric domains under varying bias voltages. As the voltage increases, the ferroelectric domain undergoes gradual contraction or dilation accompanied by an increase in boundary curvature. The schematic representation (Fig. 1d and e) further elucidates this mechanism. Under the influence of the electric field, domain wall motion is restricted by the topological protection provided by the nodal regions of the moiré superlattice. Specifically, since these nodal regions are non-ferroelectric and cannot be polarized, the adjustment of the ferroelectric domains is accomplished only via curvature modulation. Notably, under extremely high electric fields, two high-curvature domain walls can approach each other closely, and the polarization region opposite to the field direction remains partially preserved. This behavior is fundamentally distinct from the complete polarization reversal typically seen in conventional ferroelectric domains, and the resulting unique topological configuration has been termed the "Double Domain Wall (DDW)" or "Perfect Screw Dislocation (PSD)" (Fig. S7 online) [18].

Through quantitative analysis of the ferroelectric domain area S and domain wall curvature K as a function of applied bias (Fig. 1f, with domain wall marked by red dashed lines in Fig. 1c), we identify two distinct stages of evolution. First, S decreases continuously without abrupt switching, which is consistent with the previously reported voltage-dependent evolution of the XM/MX region ratio in macroscopic moiré polar networks [6]. Then, a transition near ~6 V is observed, where K begins to rise more sharply while S continues its monotonic decrease, this voltage corresponds to the threshold for DDW formation. Beyond this critical value, the emergence of the DDW structure introduces an energy barrier to further polarization, necessitating a substantial increase in domain wall curvature to overcome this state. The theoretically calculated threshold voltage of ~5.74 V (Fig. S8 online) exhibits excellent consistency

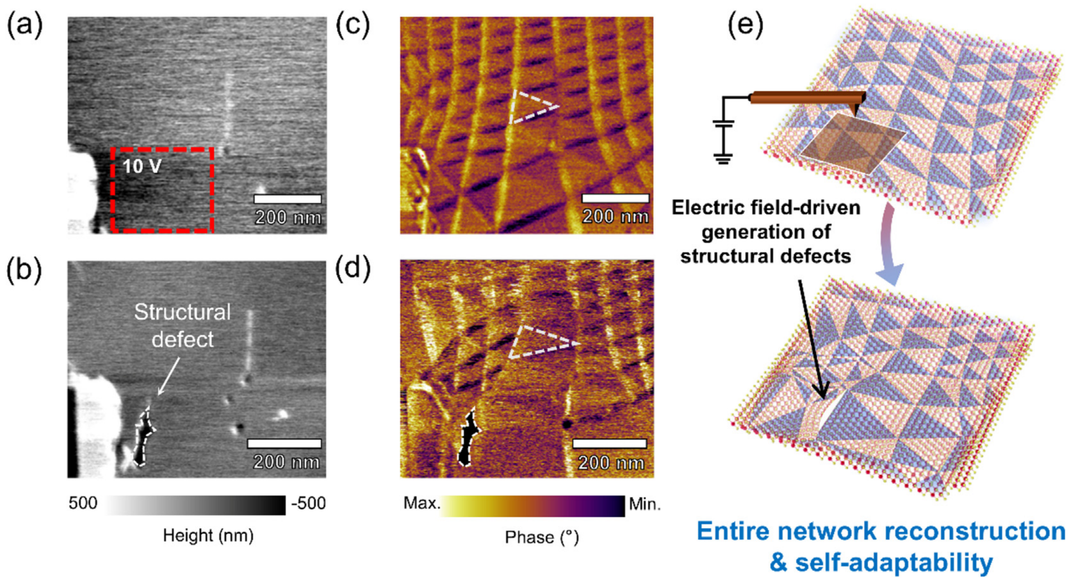

Fig. 2. The self-adaptability of the moiré polar network after electric-field-induced structural defects. (a) Morphology image and (b) phase map before the structural defects, with the region affected by the electric field highlighted by red dashed lines, (c) topography image and (d) phase map after electric field loading. (e) Reconstruction of the moiré polar network following structural defects.

with the experimental results. Furthermore, the electric field exerts minimal influence on the moiré polar network on the hBN substrate, likely due to the shielding effect of its high dielectric constant (Fig. S9 online). Moiré polarization switching is non-volatile (Fig. S10 online) and can be locally induced without perturbing adjacent regions (Fig. S11 online). This behavior is analogous to conventional ferroelectrics in enabling local domain writing, while also exhibiting additional topological protection.

Given the high sensitivity of moiré polar networks to stacking configurations, we designed an electric-field-induced perforation experiment in tBL-MoS_2 to verify the impact of structural defects on polarization distribution. By increasing the time during which voltage is applied to each unit area, localized physical damage, hereafter referred to as structural defects, can be introduced. Fig. 2a, b, and Fig. S12a, b (online) present the surface topography evolution before and after localized electric field modulation (10 V DC bias within the red dashed regions), revealing multiple electrically induced engineered defect features. Notably, the mappings before and after perturbations (Fig. 2c, d, and Fig. S12c, d online) indicate that the moiré superlattice undergoes global reconstruction. Specifically, these mappings reveal widespread changes in the moiré periodicity and domain wall orientations across the entire imaged area, not just confined to the vicinity of the induced defect. For example, compared to Fig. 2c, one can see not only the disappearance of the ferroelectric domain at the defect site in Fig. 2d, but also a reorientation of the ferroelectric domains (e.g., the triangular domain marked by white dashed lines in Fig. 2c and d), indicating a collective response of the superlattice. This demonstrates that even when partial structural defects occur, the moiré polar network undergoes global restructuring to preserve its distinctive polarization distribution and adapt to the altered structural conditions (Fig. 2e). The self-adaptive property enables moiré ferroelectric devices to maintain normal overall logical functionality, even when subjected to local perturbations during operation.

To elucidate the mechanism underlying the formation of morphological changes, a topographic profile was extracted (Fig. S13b online), yielding a measured depression depth of 636 pm, close to the theoretical thickness of a single MoS_2 layer, indicating cross-layer structural penetration. Combined with other cases of field-induced morphological changes (Fig. S13 online), Fig. S14 (online) illustrates the following mechanism: although the artificial stacking effectively establishes small-angle moiré polar coupling, gaseous impurities trapped within the van der Waals gaps undergo electric-field-induced migration and localized aggregation under strong fields. When the electric field exceeds a critical threshold, the resulting stress triggers film rupture. It is noteworthy that all observed morphological variations exhibit a distinct asymmetry (valley-ridge-like), which is related to the tangential force components introduced during dynamic scanning probe modulation, a phenomenon that was not observed in static point polarization experiments (Fig. S15 online). While interlayer-encapsulated gas molecules do not compromise interlayer polar coupling, they may elevate dielectric breakdown risks in moiré-based devices. Future moiré-based devices may necessitate enhanced interfacial cleanliness protocols, such as adopting vacuum-based encapsulation processes.

In summary, we elucidate the dynamic behavior of ferroelectric domains and the self-adaptive nature of moiré polar networks within tBL-MoS_2-derived superlattices. The experiments demonstrate that moiré ferroelectric domains can be locally controlled by electric fields. Under topological protection from nodal regions, the polarization reversal of triangular domains proceeds via curvature modulation, where two edges converge to form a DDW structure once a critical voltage is reached. During electric field modulation, moiré polar networks undergoing local structural perturbations reconstruct globally to preserve their polarization configuration. These findings reveal the unique evolution and adaptive reconstruction of moiré polarization under electric fields, and the topologically protected dynamics offer valuable insights for 2D device design while providing scientific guidance for low-power, high-stability applications.

Conflict of interest

The authors declare that they have no conflict of interest.

Acknowledgments

This work was supported by the National Natural Science Foundation of China (52272135, 62375020, 92163206, and 62274010), the National Key Research and Development Program of China

(2022YFA1403302, 2021YFA1400100, and 2020YFA0308800), the Young Elite Scientists Sponsorship Program by CAST (2023QNRC001), the Beijing Natural Science Foundation (Z19J00015), the CAS Youth Interdisciplinary Team, Beijing National Laboratory for Condensed Matter Physics (2024BNLCMPKF003), and the Fundamental Research Funds for the Central Universities (2023CX01030).

Author contributions

Yeliang Wang, Yuan Huang, and Jiakai Wang conceived the overall experimental research plan. Jiakai Wang was responsible for experimental preparation, material characterization, and data analysis. Xu Han, Guanchu Liu, Zihao Guo, Longshuo Gu, Jiahao Yan, Shiqi Yang, Chunsheng Hu, Chicheng Liu, Yunyun Dai, and Xia Liu participated in result discussions and manuscript editing.

Appendix A. Supplementary material

Supplementary data to this article can be found online at https://doi.org/10.1016/j.scib.2025.06.026.

References

[1] Nuckolls KP, Yazdani A. A microscopic perspective on moiré materials. Nat Rev Mater 2024;9:460–80.
[2] Xu HJ, Liu YZ, Finocchio G, et al. Progress and perspective on the topological spin textures in two-dimensional van der Waals magnets. Sci Bull 2024;69:1612–6.
[3] Yasuda K, Wang XR, Watanabe K, et al. Stacking-engineered ferroelectricity in bilayer boron nitride. Science 2021;372:1458–62.
[4] Wang XR, Yasuda K, Zhang Y, et al. Interfacial ferroelectricity in rhombohedral-stacked bilayer transition metal dichalcogenides. Nat Nanotechnol 2022;17:367–71.
[5] Van Winkle M, Dowlatshahi N, Khaloo N, et al. Engineering interfacial polarization switching in van der Waals multilayers. Nat Nanotechnol 2024;19:751–7.
[6] Ko K, Yuk A, Engelke R, et al. Operando electron microscopy investigation of polar domain dynamics in twisted van der Waals homobilayers. Nat Mater 2023;22:992–8.
[7] Wang L, Qi JJ, Wei WY, et al. Bevel-edge epitaxy of ferroelectric rhombohedral boron nitride single crystal. Nature 2024;629:74–9.
[8] Weston A, Castanon EG, Enaldiev V, et al. Interfacial ferroelectricity in marginally twisted 2D semiconductors. Nat Nanotechnol 2022;17:390–5.
[9] McGilly LJ, Kerelsky A, Finney NR, et al. Visualization of moiré superlattices. Nat Nanotechnol 2020;15:580–4.
[10] Zhang S, Liu Y, Sun ZY, et al. Visualizing moiré ferroelectricity via plasmons and nano-photocurrent in graphene/twisted-WSe_2 structures. Nat Commun 2023;14:6200.
[11] Ding J, Xiang HX, Zhou WQ, et al. Engineering band structures of two-dimensional materials with remote moiré ferroelectricity. Nat Commun 2024;15:9087.
[12] Wan SY, Huang HY, Liu HL, et al. Intertwined flexoelectricity and stacking ferroelectricity in marginally twisted hBN moiré superlattice. Adv Mater 2024;36:2410563.
[13] Li Y, Wan SY, Liu HL, et al. Topological polar networks in twisted rhombohedral-stacked bilayer WSe_2 moiré superlattices. Nano Lett 2024;24:13349–55.
[14] Ding PF, Yan JH, Wang JK, et al. Manipulation of moiré superlattice in twisted monolayer-multilayer graphene by moving nanobubbles. Nano Lett 2024;24:8208–15.
[15] Molino L, Aggarwal L, Enaldiev V, et al. Ferroelectric switching at symmetry-Broken interfaces by local control of dislocations networks. Adv Mater 2023;35:2207816.
[16] Cao Y, Luo JY, Fatemi V, et al. Superlattice-induced insulating states and valley-protected orbits in twisted bilayer graphene. Phys Rev Lett 2016;117:116804.
[17] Kim K, Yankowitz M, Fallahazad B, et al. Van der Waals heterostructures with high accuracy rotational alignment. Nano Lett 2016;16:1989–95.
[18] Halbertal D, Finney NR, Sunku SS, et al. Moiré metrology of energy landscapes in van der Waals heterostructures. Nat Commun 2021;12:242.